

# Hydrodynamic Forces acting on Two Flexible Free-hanging Cantilevers in Tandem Configurations due to Cross-flows

Rudi Walujo Prastianto<sup>1</sup>

**Abstract**—The experimental study has been performed on two flexible free-hanging circular cantilevers in tandem configurations subjected to uniform cross-flows. The experiment was intended to investigate the time-dependent forces characteristics acting on the cylinders due to Vortex-Induced Vibration (VIV) phenomenon. The tests cylinders have free bottom-end conditions and can freely oscillate. The motions of the cylinders are evaluated as a bidirectional motion, in-line and transverse to the flow. Each cylinder has a length-to-diameter ratio of 34.4 with a low mass ratio of about 1.24. Based on cylinder's diameter and free-stream flow velocities, the Reynolds number varied from 10,800 to 37,800. For examining Wake Induced Vibration (WIV) on the induced forces characteristics, five different gaps between the cylinders were employed. New various findings indicated that the dynamics of the present two free-hanging cantilever cylinders in tandem configurations are unique and definitely different to those other tandem configurations of either, two stationary cylinders or a transverse-only motion downstream cylinder lies behind a stationary upstream one.

**Keywords**—Free-hanging cantilevers, tandem configurations, cross-flow, Vortex Induced Vibration (VIV), free bottom-end condition, bidirectional motion, Wake Induced Vibration (WIV).

## I. INTRODUCTION

In order to increase the productivity, future floating Ocean Thermal Energy Conversion (OTEC) or Carbon Dioxide (CO<sub>2</sub>) sequestration platforms may have multiple, two or more, Cold Water Pipes (CWP) or CO<sub>2</sub> injection pipes. If so, it obviously needs more “clear picture” on the physical mechanism of interaction among the pipes due to the current. One possible basic configuration in such multiple riser system is a tandem configuration of two cylinders. Therefore, better understandings on the dynamics behavior of such free-hanging risers in a tandem configuration due to water flows are indeed required, particularly for the design purpose of those types of structures.

Simply, when two cylinders are free to oscillate due to current flows, the wake interference between them gains much more complex as well as response of the downstream cylinder. The wake of the upstream cylinder impinging on the downstream cylinder differs from the case of stationary cylinders. In turn, the response of the downstream cylinder differs from both that of a single and a cylinder in the wake of a fixed cylinder. Based on such complexity, some phenomena which are still not clearly understood are needed to be clarified, such as the

characteristics of time-dependent fluid forces acting on the cylinders.

Regarding the fluid-cylinder interaction characteristics of two circular cylinders in tandem arrangements subjected to cross-flows, several experimental works have been done over the years from a variety of perspectives [1-8]. Xu and Zhou [6] studied the Strouhal number ( $St$ ) of two static cylinders in tandem configurations within relatively wide range of Reynolds number ( $Re$ ) and gap between the cylinders,  $L_{UD}$ . They found a strong dependency of the  $St$  on the  $Re$  and  $L_{UD}$ . The way in which the  $St$  varies with the gap depends on the flow regime, while the  $St-Re$  relationship is classified into four categories, based on their behaviors which are associated with distinct flow physics.

Another work by Alam et al. [4] evaluated fluctuating fluid forces in a tandem configuration of two stationary circular cylinders. They observed that the fluctuating lift and drag acting on the downstream cylinder are very sensitive to the cylinders gap, particularly which is smaller than the critical gap of  $L_{UD} = 4D$ . Meanwhile, for a long flexible cylinder located in the wake of a stationary geometrically similar cylinder as a tandem configuration, Brika and Laneville [2, 3] reported that for  $L_{UD} = 7D$  and  $8.5D$ , the downstream cylinder exhibits a combination of vortex-induced and wake-galloping oscillations.

More recent studies examined two vertically tandem cylinders with a fixed upstream and transverse-direction allowable oscillation only downstream cylinder. The results confirmed that the downstream cylinder peak amplitude was about 50% higher than that experienced by a single cylinder and the galloping-like phenomenon occurred in the gap range of  $3D < L_{UD} < 5.6D$ . Meanwhile, it was predicted that high amplitude oscillation experienced by the downstream cylinder was due to excitation by the vortex component of the lift force at higher reduced velocity [9, 10].

In particular, this paper presents the results of experiment which is addressed to evaluate wake interference effects on the induced forces characteristics of two free-hanging cylindrical cantilevers in tandem configurations due to uniform water cross-flows, by making some variations on the gap between the cylinders. The cylinders motions have been studied in [14].

## II. EXPERIMENTAL CONDITIONS

### A. Experimental Setup

The experiment outlined in this paper is a part of an experiment series on the flow-induced vibration of free-hanging circular cantilevers. The test has been carried out in a towing tank of the Department of Marine System

<sup>1</sup>Rudi Walujo Prastianto is Department of Ocean Engineering, Faculty of Marine Engineering, Institut Teknologi Sepuluh Nopember, Surabaya, 60111, Indonesia.

Engineering at Osaka Prefecture University, Japan. The tank has a total length of 70.0 m with effective running distances of about 45 m, 3.0 m wide and the depth of 1.5 m. The tank is equipped by a main towing carriage with a maximum towing speed of 2.5 m/sec.

Each test cylinder is made of standard polyvinyl chlorite (PVC) pipe with a total length of 1.65 m, outside diameter ( $D$ ) of 48 mm, wall thickness of 4 mm, and mass per unit length in air of 0.764 kg/m. Each cylinder has a total aspect ratio (total length-to-diameter ratio) of 34.4, and the mass ratio (the ratio of cylinder mass to displaced water mass) of about 1.24. The ratio of the cylinder diameter to tank width was 16:1000, so that some disturbances coming into the system due to the tank's wall (e.g. reflection wave, etc) are can be neglected. The top-end of each cylinder is connected to a 2-component load cell which is fixed to adjustable beams mounted on the towing carriage (Fig. 1(a)). The load cells are used for measuring the hydrodynamic forces acting on the test cylinders in both in-line (drag force) and transverse (lift force) directions, simultaneously. Meanwhile, to measure the inline and transverse motions of the cylinders, small dimension of 1-direction waterproof accelerometers (Kyowa ASW-A type) are installed inside the bottom-end of the cylinders: two accelerometers for the downstream cylinder, and one accelerometer for the upstream cylinder. Each accelerometer has approximately 40 grams of weight excluded the cable, 18×18×24 mm in dimensions, and up to 490.3 kPa of water pressure resistance.

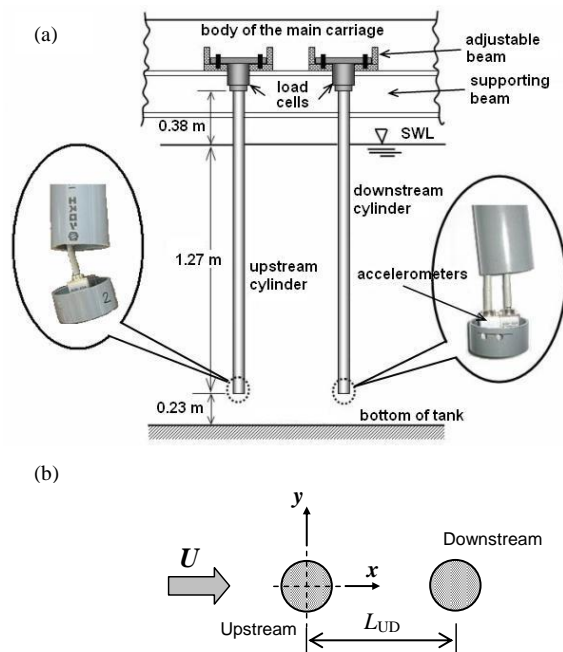


Fig. 1. (a) Schematic view of the experimental setup (side view) for the tandem configuration, (b) nomenclature for the tandem configurations of two flexible free-hanging circular cantilevers of equal diameter immersed in uniform cross-flows

As an initial condition, the cylinders are partially submerged (wet length = 1.27 m, to give a wet aspect ratio of 26.5 for each cylinder) into the still water from a towing carriage as hanging vertical cantilevers with 0.23 m gap (allowing 3-dimensional effect of the flow around the cylinders' bottom-end) from the bottom of the tank. To investigate interference effects on the induced forces

acting on the test cylinders, tandem configurations of two cylinders with five different center-to-center gaps ( $L_{UD}$ ) of  $5D$ ,  $7D$ ,  $9D$ ,  $10D$ , and  $12D$ , were considered. Fig. 1 illustrates the experimental setup and a schematic plan view of the tandem configurations.

To generate uniform cross-flows, the carriage is moved along the tank with the test cylinders fixed to the carriage. During the towing for each case of the test, the cylinders behave as self-excited motion in 2 degrees of freedom. The towing speeds are changed from 0.20 up to 0.70 m/sec by increments of 0.05, which approximately corresponds to the Reynolds number of 10,800 ~ 37,800. The Reynolds number is defined as  $Re = UD/\nu$ , where  $\nu$  is the kinematics viscosity of the water. The kinematics viscosity is assumed to be  $0.89 \times 10^{-6} \text{ m}^2/\text{sec}$  for this experiment. Thus, the parameters of the test include the towing speed ( $U$ ) and relative position between the cylinders ( $L_{UD}$ ); to form a total of 55 cases.

### B. Data Acquisition and Processing

The data were acquired through a standard data acquisition system with sampling rate of 50 Hz and low-pass filtered by a frequency of 20 Hz. A total of seven channels were used to collect these forces and response data for both upstream and downstream cylinders. The raw signals are digitally low-pass filtered by a cut-off frequency of 6 Hz in order to isolate the low modes. The data used for the calculation of the measured parameters are based on a selected range of approximately stationary data within the whole duration of the towing for each case.

Relationships among the total, mean, and oscillating part of the measured forces are treated as  $F_D = F_{D,mean} + F_{D,osc}$  and  $F_L = F_{L,mean} + F_{L,osc} = 0 + F_{L,osc} = F_{L,osc}$ , where  $F_D$  and  $F_L$  are the total force,  $F_{D,mean}$  and  $F_{L,mean}$  are the mean part, and  $F_{D,osc}$  and  $F_{L,osc}$  are the oscillating part of the drag and lift force, respectively [11]. In the case of lift force, the mean part is always assumed to be zero. The related total drag ( $C_{D,rms}$ ), oscillating drag ( $C_{D,osc,rms}$ ), and lift coefficients ( $C_{L,rms}$ ) are then calculated by normalizing each corresponding term of force by  $0.5\rho U^2 DL_w$ , in which their root mean square (*rms*) values are considered. The  $\rho$  is water density ( $1,000 \text{ kg/m}^3$ ),  $U$  is free-stream uniform flow velocity (or towing speed),  $D$  is cylinder diameter, and  $L_w$  serves as the test cylinder's wet length. Well known Fast Fourier Transform (FFT) procedure is applied to analyze the forces' frequency content. The forces' coefficients and frequencies are presented as a function of reduced flow velocity, which is defined as  $Ur = U/f_{n,w}D$ , with  $f_{n,w}$  being the fundamental (1<sup>st</sup> mode) natural frequency of the cylinders in still water.

Several free decay tests are performed in order to measure the fundamental natural frequencies of both two cylinders used in the present test. Each cylinder has a different number of accelerometers installed inside it, thus has slightly different total mass. To ensure the consistency of results, the decay tests are performed 4 times in air and 3 times in water for each cylinder. Some of the tests in air condition are carried out in both  $x$  and  $y$  directions, to check the uniformity of the natural frequencies in those two directions. The tests produce unidirectional mean values of the fundamental natural frequency in both air and water conditions. They are 4.30

Hz and 2.10 Hz for the upstream cylinder, and 4.20 Hz and 2.15 Hz for the downstream cylinder. There was approximately 50% decrease on the cylinder's natural frequency of each cylinder for the still water case.

III. RESULTS AND DISCUSSION

A. Hydrodynamic Force Coefficients

It is found that characteristics of the forces acting on the downstream cylinder in the tandem configurations are completely different than that of the single cylinder case. Coefficients of the total drag, lift, mean drag, and oscillating drag are shown in Fig. 2~5, respectively. All coefficients have strong dependency on the  $Ur$  and  $L_{UD}$  parameters. Fig. 2 and 3 respectively show the coefficients of the total drag and lift for the downstream cylinder. For all  $L_{UD}$  at  $Ur \leq 3.47$ , the  $C_{D,rms}$  are relatively larger, and then starting to softly decline as the  $Ur$  increases. There is a similarity among each other pattern of the coefficients as a function of the  $Ur$  at different  $L_{UD}$ , even each different in magnitude.

At the same time, the  $C_{L,rms}$  for all  $L_{UD}$  basically increases with the  $Ur$  (Fig. 3). At first two gaps ( $L_{UD} = 5D$  and  $7D$ ), the coefficients data relatively increase with

the  $Ur$  as linear functions. But for the 3 remaining  $L_{UD}$  values, the data do not follow the linear function any more. The relationship between the  $C_{L,rms}$  and  $Ur$  becomes more complicated. For all  $L_{UD}$  values, at  $Ur > 5.33$ , the  $C_{L,rms}$  tends to increase that in contrast to the single cantilever case (see Fig. 6), and the increasing slope then becomes smaller as the  $L_{UD}$  increases. The  $C_{L,rms}$  values gradually decrease with increasing the  $L_{UD}$ , particularly Cubic polynomial functions can fit up the  $C_{D,mean}$  data with best accuracy for each  $L_{UD}$  as shown in Fig. 4. In general, as the  $L_{UD}$  increases, the  $C_{D,mean}$  values regularly become larger, particularly at a range of  $Ur \leq 5.33$ . However, as the  $Ur$  increases, the  $C_{D,mean}$  tends to reach a constant value and at the highest  $Ur$ , the  $C_{D,mean}$  has almost same values of about 0.04 for all  $L_{UD}$ . It means that at highest  $Ur$ , the  $C_{D,mean}$  is independent of the  $L_{UD}$  parameter within the regime of high  $Ur$ .

Meanwhile, the influence of the  $L_{UD}$  parameter on the  $C_{D,osc,rms}$  can be seen in Fig. 5. As the  $L_{UD}$  increases, the coefficients in the range of  $3.97 \leq Ur \leq 6.79$  gradually drop into their lowest values and then almost constant with the  $Ur$ ; independent of the  $Ur$ , particularly at the largest gap ( $L_{UD} = 12D$ ).

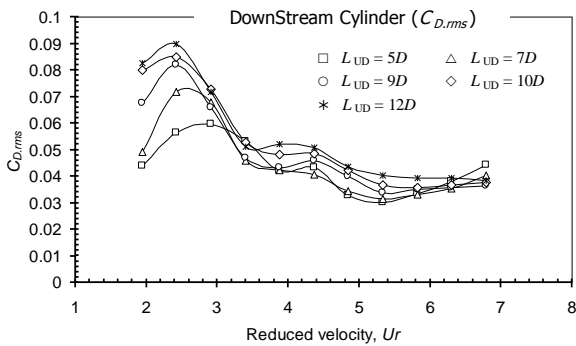


Fig. 2. Total drag coefficients of the downstream cylinder in tandem configurations (all cases)

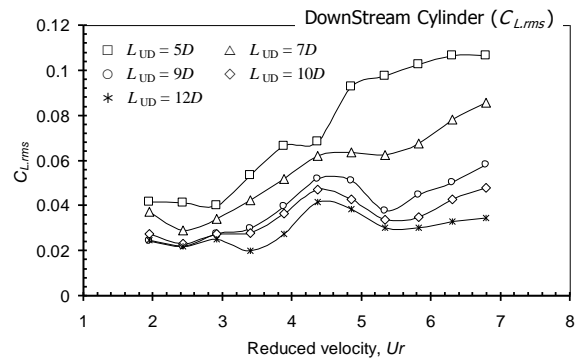


Fig. 3. Lift coefficients of the downstream cylinder in tandem configurations (all cases)

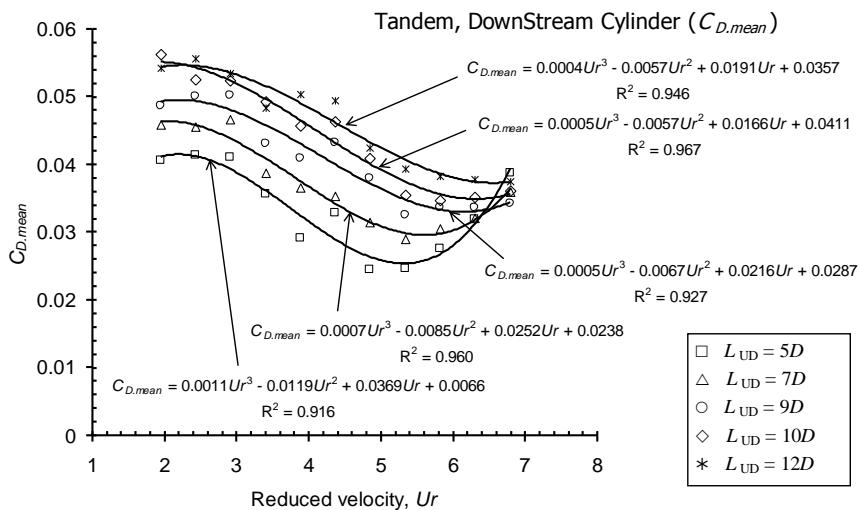


Fig. 4. Mean drag coefficients of the downstream cylinder for all cases in tandem configurations. The lines represent approximation curves of the coefficients for each case

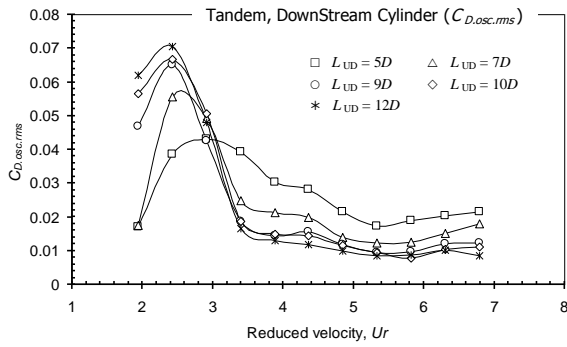


Fig. 5. Oscillating drag coefficients of the downstream cylinder for all cases

For the upstream cylinder, on the other hand, the forces coefficients indicate relatively similar characteristics to the single cylinder case as displayed in Fig. 6 and 7. Fig. 6 is for the total drag and lift, and Fig. 7 is for the mean and oscillating drag. As the  $L_{UD}$  increases, the values and distribution of the coefficients as a function of the  $Ur$  gradually follow the characters of the single cylinder case. It suggests that the dynamics of the downstream cylinder gradually has weaker effect to the upstream one, as the gap is getting larger.

It is important to introduce here, another existing interference experiment carried out with a stationary upstream cylinder for a comparison purpose. For instance, Assi et al., [9] performed experimental works of a transverse-only motion downstream cylinder located behind a stationary upstream one in a tandem arrangement. The bottom-end of the cylinders is conditioned such as the 2-dimensional flow exists along the cylinders' span, by making a tiny gap between the bottom-end of the cylinders and the tunnel floor. In a lower range  $Re$  condition of 3,000 to 13,000, they reported that the transverse peak amplitude of the downstream cylinder is about  $1.4D$ , occurs at a gap of  $3D$ , which is 50% higher than the maximum amplitude observed for the single cylinder case. It means that at such condition, the lift force acting on the downstream cylinder is larger than that for the single transverse-only motion cylinder.

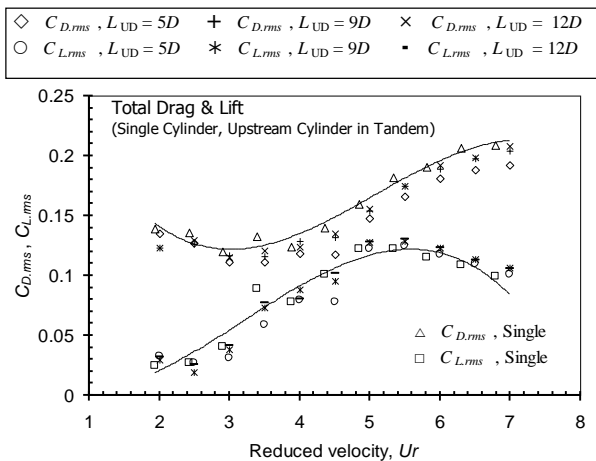


Fig. 6. Total drag and lift coefficients of the upstream cylinder in tandem configurations. A comparison to the single case, for some tandem cases with  $L_{UD} = 5D, 9D,$  and  $12D$ . The lines represent approximation curves for the coefficients of the single cylinder case

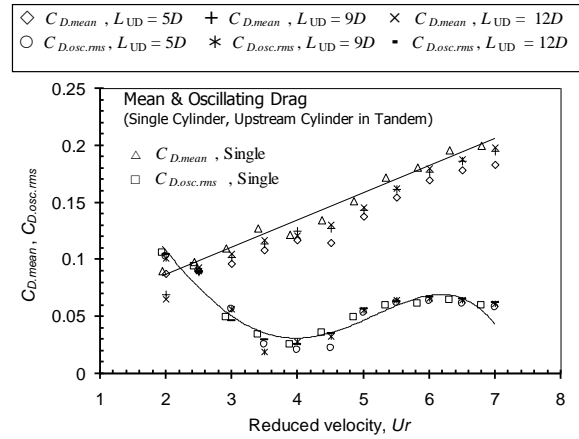


Fig. 7. Mean and oscillating drag coefficients of the upstream cylinder in tandem configurations. A comparison to the single case, for some tandem cases with  $L_{UD} = 5D, 9D,$  and  $12D$ . The lines represent approximation curves for the coefficients of the single cylinder case

It is interesting to note that different features on the dynamics of the downstream cylinder in the present test compared to the existing work in [9], can be expected as the effects of an oscillating upstream cylinder, moreover with free-end bottom conditions. Larger wake area created by the oscillating upstream cylinder as the transverse motion increases, significantly reduces the lift acting on the downstream cylinder, and in turn suppresses its response.

B. Hydrodynamic Force Frequencies

Power Spectral Density (PSD) of the drag and lift forces as a function of the  $Ur$  for some representative cases in the tandem configurations ( $L_{UD} = 5D, 9D,$  and  $12D$ ) are depicted in Fig. 8~10. From the plots, the frequency content, change on the magnitude and peak of the drag and lift for both the upstream and downstream cylinders as a function of the  $Ur$  and  $L_{UD}$  can be recognized. In the PSD plots, however, some frequencies for low  $Ur$  can not be seen due to their relatively very small peaks.

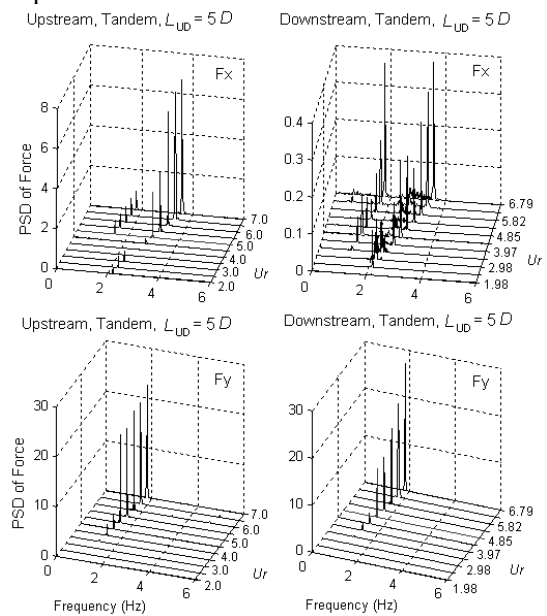


Fig. 8. Spectra of the drag ( $F_x$ ) and lift ( $F_y$ ) acting on the cylinders, tandem configurations,  $L_{UD} = 5D$

In the plots of the drag ( $F_x$ ) frequencies for both the upstream and downstream cylinders, for each  $Ur$ , there are a couple of dominant frequencies which the second frequency indicates the drag frequency itself, while the first one represents the corresponding lift frequency. For the downstream cylinder, at larger  $L_{UD}$ , as the  $Ur$  increases, the second frequencies step by step relatively become weaker as shown in Fig. 10 at  $L_{UD} = 12D$ . Meanwhile, the lift frequencies (Fig. 8-10) at higher  $Ur$  almost consistently have only a single frequency for both the upstream and downstream cylinders, even the peaks decrease as the  $L_{UD}$  increases. These indicate that at large  $L_{UD}$  and  $Ur$ , the drag acting on the downstream cylinder becomes smaller and oppositely, the lift becomes larger, as previously shown by Fig. 2 or 5 and Fig. 3. Consequently, the downstream cylinder oscillates as transverse-dominated motions, as can be confirmed by the motion data of the downstream cylinder that has been studied in [14].

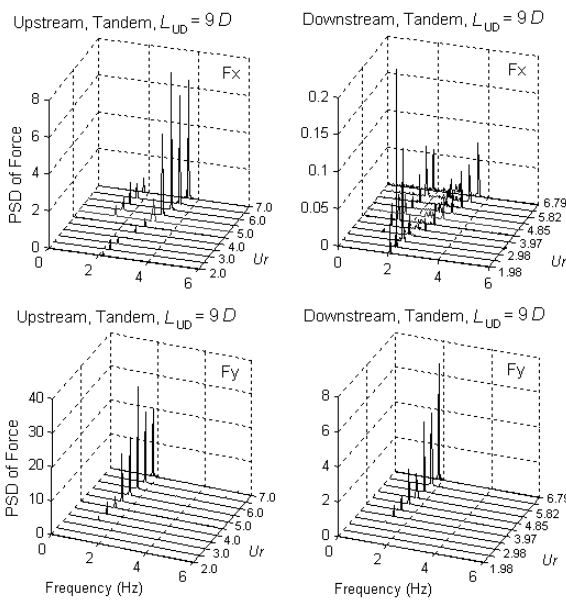


Fig. 9. Spectra of the drag ( $F_x$ ) and lift ( $F_y$ ) acting on the cylinders, tandem configurations,  $L_{UD} = 9D$

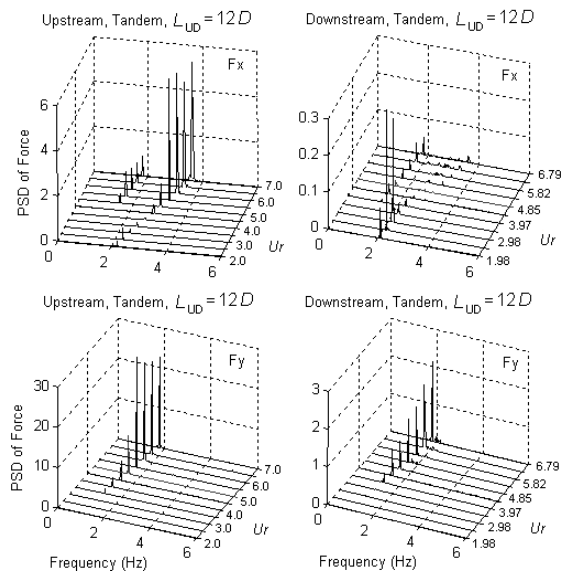


Fig. 10. Spectra of the drag ( $F_x$ ) and lift ( $F_y$ ) acting on the cylinders, tandem configurations,  $L_{UD} = 12D$

The summary of the drag and lift frequencies ( $f_D$  and  $f_L$ ) for the upstream and downstream cylinders in the tandem configuration is plotted as function of the  $Ur$  in Fig. 11-13, in term of their non-dimensional frequencies for  $L_{UD} = 5D, 9D$ , and  $12D$ , respectively. The frequencies values plotted are the predominant frequencies taken from their PSD that are normalized by the fundamental natural frequency of each cylinder in still water condition ( $f_{n,w}$ ).

The frequencies of the forces change almost linearly with the  $Ur$  in the range used. Substantially, around the  $Ur \geq 3.0$ , the drag-lift ratios are approximately constant at a value of 2. But, within  $Ur < 3.0$ , the ratios become larger

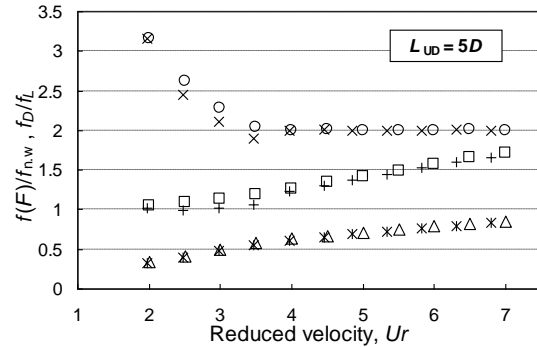


Fig. 11. Non-dimensional frequencies of the drag and lift forces for the upstream and downstream cylinders, a tandem configuration,  $L_{UD} = 5D$ .  $\square$  and  $\triangle$ ,  $f_D/f_{n,w}$  and  $f_L/f_{n,w}$  for upstream cylinder;  $+$  and  $*$ ,  $f_D/f_{n,w}$  and  $f_L/f_{n,w}$  for downstream cylinder;  $\circ$  and  $\times$ ,  $f_D/f_L$  for upstream and downstream, respectively

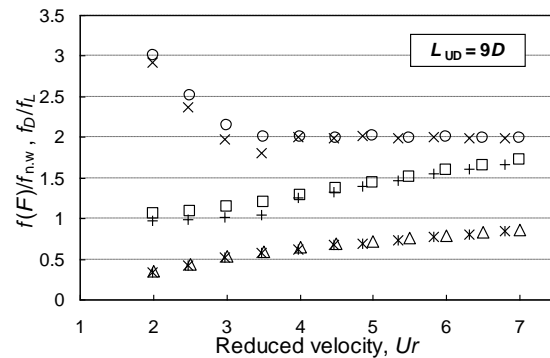


Fig. 12. Non-dimensional frequencies of the drag and lift forces for the upstream and downstream cylinders, a tandem configuration,  $L_{UD} = 9D$ .  $\square$  and  $\triangle$ ,  $f_D/f_{n,w}$  and  $f_L/f_{n,w}$  for upstream cylinder;  $+$  and  $*$ ,  $f_D/f_{n,w}$  and  $f_L/f_{n,w}$  for downstream cylinder;  $\circ$  and  $\times$ ,  $f_D/f_L$  for upstream and downstream, respectively

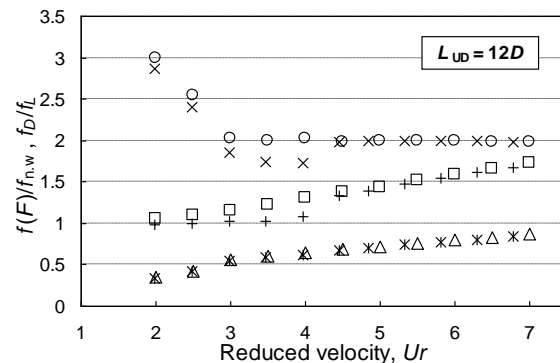


Fig. 13. Non-dimensional frequencies of the drag and lift forces for the upstream and downstream cylinders, a tandem configuration,  $L_{UD} = 12D$ .  $\square$  and  $\triangle$ ,  $f_D/f_{n,w}$  and  $f_L/f_{n,w}$  for upstream cylinder;  $+$  and  $*$ ,  $f_D/f_{n,w}$  and  $f_L/f_{n,w}$  for downstream cylinder;  $\circ$  and  $\times$ ,  $f_D/f_L$  for upstream and downstream, respectively

than 2, which are about 3 and 2.5 at  $Ur \approx 2.0$  and 2.5, respectively. At approximately  $Ur \leq 4.0$ , however, as the  $L_{UD}$  increases, the drag frequencies of the downstream cylinder gradually deviate larger from the upstream values. Other cases in these tandem configurations show similar characteristics on the forces' frequency content. Therefore, this demonstrates that the interaction between the cylinders in these tandem configurations gives no effects on the change of the forces frequencies or drag-lift ratios.

The results from these tandem tests also have proved that the ratios between the drag and lift frequencies for both upstream and downstream cylinders are independent of the  $Ur$  and  $L_{UD}$  within the high  $Ur$ , as occurred in the cases of a single cantilever [12] and the triangular configurations of 3 free-hanging cantilevers [13] that have been previously studied.

In a tandem configuration of two static-rigid cylinders, Xu and Zhou [6] found that at the  $L_{UD} > 5D$ , the flow physic around the cylinders is characterized by co-shedding only. Within this gap, the vortices shed from the upstream as well as the downstream cylinder have identical frequencies. The Strouhal number ( $St$ ) increases with increasing the gap, approaches a constant between 0.18 and 0.22, a typical value of the  $St$  for a stationary cylinder, for  $L_{UD} > 10D$ . This phenomenon means that at  $L_{UD} > 10D$ , each cylinder behaves as the single cylinder; the wake interference is no longer exists. This fact is in contrast to the evidence observed in the present test. Due to the oscillation of the upstream cylinder, the characteristics of the downstream cylinder are never approaching to that for the single cylinder one, in term of the forces acting on it, although the gap  $L_{UD} > 10D$ .

Apparently, a fluid-structure interaction mechanism which is responsible to the observed behavior in tandem cases can be addressed to the *wake-induced vibrations* (WIV) term. Interference between vortex shedding from the upstream cylinder and the own shedding frequency from VIV of the downstream cylinder could be able to create two consequences: amplify or oppositely suppress the dynamics of the downstream cylinder. Based on the evidences observed in present tandem cases, the second consequent is the case. The oscillating upstream cylinder creates wider wake area behind the cylinder at higher  $Ur$  (for  $Ur \geq 3.47$ ), due to larger transverse amplitudes generated by a coupled inline-transverse motion as also mentioned in [15, 16], as a consequence of the bidirectional motion. The wake almost completely covers the downstream cylinder, creates a shielding effect; in turn changes and reduces the vicinity flow pattern and velocity. The lower flow velocities produce smaller forces acting on the downstream cylinder that finally suppress the cylinder's motion in both inline and transverse directions. Until at the largest gap tested,  $L_{UD} = 12D$ , the influence of the upstream cylinder still strong.

Finally, such various findings gave us insights that the dynamics of the present two flexible free-hanging cantilever cylinders in tandem configurations are unique and definitely different to those other tandem configurations of either, two stationary cylinders or a transverse-only motion downstream cylinder lies behind a stationary upstream one. At least, the parameters of bidirectional motion inline and transverse to the flow,

free bottom-end condition of the cylinders, and a range of the  $Re$ , simultaneously affect the induced forces characteristics acting on the cylinders.

#### IV. CONCLUSIONS

From the present experimental study, some conclusions can be drawn as follows:

1. Characteristics of the forces acting on the downstream cylinder in the tandem configurations are completely different from that of the single cylinder case. For all the gap between the cylinders,  $L_{UD}$ , at low reduced velocity,  $Ur$ , the total drag coefficient,  $C_{D,rms}$ , gradually increases and then at  $Ur \geq 3.47$ , the  $C_{D,rms}$  starting to moderately decline with the  $Ur$ . At the same time, the total lift coefficient,  $C_{L,rms}$ , for all  $L_{UD}$  basically increases with the  $Ur$ . For all  $L_{UD}$  values, at  $Ur > 5.33$ , the  $C_{L,rms}$  tends to increase that in contrast to the single cantilever case, and the increasing slope then becomes smaller as the  $L_{UD}$  increases.
2. The mean drag coefficient,  $C_{D,mean}$ , becomes larger as the  $L_{UD}$  increases, particularly within  $Ur \leq 5.33$ . However, as the  $Ur$  increases, the  $C_{D,mean}$  tends to reach a constant value and at the highest  $Ur$ , the  $C_{D,mean}$  has almost same values of about 0.04 for all  $L_{UD}$ ; the  $C_{D,mean}$  is independent of the  $L_{UD}$  parameter. As the  $L_{UD}$  increases, the oscillating drag coefficient,  $C_{D,osc,rms}$ , in the range of  $3.97 \leq Ur \leq 6.79$  gradually drops into their lowest values and then almost constant with the  $Ur$ ; independent of the  $Ur$ , particularly at the  $L_{UD} = 12D$ .
3. For the upstream cylinder, the forces coefficients indicate relatively similar characteristics to the single cylinder case. It suggests that the dynamics of the downstream cylinder gradually has weaker effect to the upstream one, as the gap is getting larger.
4. The frequencies of the forces change almost linearly with the  $Ur$  in the range used. Substantially, around the  $Ur \geq 3.0$ , the drag-lift ratios are approximately constant at a value of 2. But, within  $Ur < 3.0$ , the ratios are larger than 2. The interaction between the cylinders in these tandem configurations gives no effects on the change of the forces frequencies or drag-lift ratios. The results from these tandem tests also have proved that the ratios between the drag and lift frequencies for both upstream and downstream cylinders are independent of the  $Ur$  and  $L_{UD}$  within the high  $Ur$ , as occurred in the cases of a single cantilever and the triangular configurations of 3 free-hanging cantilevers that have been previously studied.
5. New various findings in the present test indicate that the dynamics of two free-hanging cantilever cylinders in tandem configurations are unique and definitely different to those other tandem configurations of either, two stationary cylinders or a transverse-only motion downstream cylinder lies behind a stationary upstream one. A term called the *wake-induced vibrations* (WIV) is responsible to the observed phenomena.



To improve our understanding to the problem, a flow visualization test is needed to be carried out further, in order to clarify the mechanism of the vortex shedding during the WIV process.

#### ACKNOWLEDGEMENTS

The author would like to thank Prof. Yoshiho Ikeda and Prof. Koji Otsuka at the Department of Marine System Engineering, Osaka Prefecture University, Japan. The author also wishes to thank Japan's Ministry of Education, Culture, Sports, Science and Technology, Indonesia's Ministry of National Education and Institut Teknologi Sepuluh Nopember (ITS), Surabaya.

#### REFERENCES

- [1] N. Mahir and D. Rockwell, 1996, "Vortex formation from a forced system of two cylinders part I: tandem arrangement", *Journal of Fluids and Structures*, Vol.10, pp. 473-489.
- [2] D. Brika and A. Laneville, 1997, "Wake interference between two circular cylinders", *Journal of Wind Eng. and Industrial Aerodynamics*, Vol.72, pp. 61-70.
- [3] D. Brika and A. Laneville, 1999, "The flow interaction between a stationary cylinder and a downstream flexible cylinder", *Journal of Fluids and Structures*, Vol.13, pp. 579-606.
- [4] Md. M. Alam et al., 2003, "Fluctuating fluid forces acting on two circular cylinders in a tandem arrangement at a subcritical Reynolds number", *Journal of Wind Eng. and Industrial Aerodynamics*, Vol.91, pp. 139-154.
- [5] D. W. Allen and D. L. Henning, 2003, "Vortex-induced vibration current tank tests of two equal-diameter cylinders in tandem", *Journal of Fluids and Structures*, Vol.17, pp. 767-781.
- [6] G. Xu and Y. Zhou, 2004, "Strouhal numbers in the wake of two inline cylinders", *Experiments in Fluids*, Vol.37, pp. 248-256.
- [7] S. J. Xu, Y. Zhou, and J. Y. Tu, 2008, "Two-dimensionality of a cantilevered-cylinder wake in the presence of an oscillating upstream cylinder", *Journal of Fluids and Structures*, Vol.24, pp. 467-480.
- [8] A. Okajima et al., 2007, "Flow-induced streamwise oscillation of two circular cylinders in tandem arrangement", *International Journal of Heat and Fluid Flow*, Vol.28, pp. 552-560.
- [9] G. R. S. Assi et al., 2006, "Experimental investigation of flow-induced vibration interference between two circular cylinders", *Journal of Fluids and Structures*, Vol.22, pp. 819-827.
- [10] G. R. S. Assi et al., 2007, "Unsteady force measurements on a responding circular cylinder in the wake of an upstream cylinder", *Proc. 26th International Conference on Offshore Mechanics and Arctic Engineering*, San Diego, USA, Paper no. OMAE 2007-29040.
- [11] M. G. Hallam, H. J. Heaf, and L. R. Wootton, 1977, "Dynamics of marine structures", *CIRIA Underwater Eng. Group, Report UR8, Atkins Research and Development*, London, UK.
- [12] R. W. Prastianto, K. Otsuka, and Y. Ikeda, 2008, "Effects of free-end condition on hydrodynamic forces of a flexible hanging-off circular cylinder undergoing vortex-induced vibration", *Proc. JASNAOE Annual Conference*, Nagasaki, Japan, pp. 259-262.
- [13] R. W. Prastianto, K. Otsuka, and Y. Ikeda, 2009, "Hydrodynamic forces on multiple free-hanging circular cantilevers in uniform flows", *International Journal of Offshore and Polar Engineering (IJOPE)*, Vol.19, No.2, pp. 108-114.
- [14] R.W. Prastianto, K. Otsuka, and Y. Ikeda, 2008, "Motion characteristics of the downstream cylinder in tandem arrangements of two self-excited flexible hanging-off circular cylinders in subcritical Reynolds numbers", *Proc. 22nd Asian-Pacific Technical Exchange and Advisory Meeting on Marine Structures (TEAM2008)*, Istanbul, Turkey, pp. 259-266.
- [15] C. P. Pesce and A. L. C. Fujarra, 2000, "Vortex-induced vibration and jump phenomenon: Experiments with a clamped flexible cantilever in water", *International Journal of Offshore and Polar Engineering (IJOPE)*, Vol.10, No.1, pp. 26-33.
- [16] A. L. C. Fujarra et al., 2001, "Vortex-induced vibration of a flexible cantilever", *Journal of Fluids and Structures*, Vol.15, pp. 651-658.